REPORT DOCUMENTATION PAGE

Form Approved
OMB No. 0704-0188

PLEASE DO NOT RETURN YOUR FORM TO THE ABOVE ORGANIZATION.

1. REPORT DATE *(DD-MM-YYYY)*	2. REPORT TYPE	3. DATES COVERED *(From - To)*
06-06-2008	Journal Article	

4. TITLE AND SUBTITLE

A Predictive Model for Satellite-derived Phytoplankton Absorption over the Louisiana Shelf Hypoxic Zone: Effects of Nutrients and Physical Forcing

5a. CONTRACT NUMBER

5b. GRANT NUMBER

5c. PROGRAM ELEMENT NUMBER

0601153N

6. AUTHOR(S)

Rebecca E. Green, Richard W. Gould

5d. PROJECT NUMBER

5e. TASK NUMBER

5f. WORK UNIT NUMBER

73-8782-07-5

7. PERFORMING ORGANIZATION NAME(S) AND ADDRESS(ES)

Naval Research Laboratory
Oceanography Division
Stennis Space Center, MS 39529-5004

8. PERFORMING ORGANIZATION REPORT NUMBER

NRL/JA/7330-07-7083

9. SPONSORING/MONITORING AGENCY NAME(S) AND ADDRESS(ES)

Office of Naval Research
800 N. Quincy St.
Arlington, VA 22217-5660

10. SPONSOR/MONITOR'S ACRONYM(S)

ONR

11. SPONSOR/MONITOR'S REPORT NUMBER(S)

12. DISTRIBUTION/AVAILABILITY STATEMENT

Approved for public release, distribution is unlimited.

13. SUPPLEMENTARY NOTES

14. ABSTRACT

We investigated environmental forcing mechanisms of phytoplankton absorption near the Mississippi River delta using multiyear satellite data. An algorithm for the phytoplankton absorption coefficient (a_{ph}) was developed from in situ measurements and applied to ocean color imagery. We employed a suite of chemical and physical forcing variables, including surface currents. For satellite-derived a_{ph} time series (2002 -2004), correlation and stepwise regression analyses revealed the most important forcing variables of a_{ph} on the Louisiana shelf. Areally, Mississippi River discharge and nitrate concentration ($[NO_3]$) were the two most important predictors of a_{ph} over the hypoxic zone (defined by its maximum extent). River discharge was important in a band stretching from the Mississippi River delta to the Louisiana-Texas border. Riverine $[NO_3]$ and wind magnitude best predicted a_{ph} in nearshore waters, and solar radiation and SST were most important farther offshore over the hypoxic zone, indicating upwelled nutrient sources to phytoplankton. A multiple linear regression model performed well in resolving seasonal and interannual a_{ph} variability in model development years (2002 -2004) (mean error of 18%, over all pixels and months) and in predicting shelf-wide a_{ph} patterns in 2005 (mean error of 32%). Our results strongly suggest that in recent years, stratification and vertical mixing, in addition to riverine $[NO_3]$, play a primary role in regulating phytoplankton biomass over the hypoxic zone. As well, a springtime model experiment showed that a_{ph} over the hypoxic zone can differ by an average absolute 37% from its average scenario owing to changes solely in environmental variables other than NO_3 flux.

15. SUBJECT TERMS

remote sensing, Louisiana shelf, phytoplankton

16. SECURITY CLASSIFICATION OF:			17. LIMITATION OF ABSTRACT	18. NUMBER OF PAGES	19a. NAME OF RESPONSIBLE PERSON
a. REPORT	b. ABSTRACT	c. THIS PAGE			Richard Gould
Unclassified	Unclassified	Unclassified	UL	17	19b. TELEPHONE NUMBER *(Include area code)* 228-688-5587

JOURNAL OF GEOPHYSICAL RESEARCH, VOL. 113, C06005, doi:10.1029/2007JC004594, 2008

A predictive model for satellite-derived phytoplankton absorption over the Louisiana shelf hypoxic zone: Effects of nutrients and physical forcing

Rebecca E. Green[1] and Richard W. Gould Jr.[1]

Received 18 October 2007; revised 11 February 2008; accepted 28 February 2008; published 6 June 2008.

[1] We investigated environmental forcing mechanisms of phytoplankton absorption near the Mississippi River delta using multiyear satellite data. An algorithm for the phytoplankton absorption coefficient (a_{ph}) was developed from in situ measurements and applied to ocean color imagery. We employed a suite of chemical and physical forcing variables, including surface currents. For satellite-derived a_{ph} time series (2002–2004), correlation and stepwise regression analyses revealed the most important forcing variables of a_{ph} on the Louisiana shelf. Areally, Mississippi River discharge and nitrate concentration ([NO_3]) were the two most important predictors of a_{ph} over the hypoxic zone (defined by its maximum extent). River discharge was important in a band stretching from the Mississippi River delta to the Louisiana-Texas border. Riverine [NO_3] and wind magnitude best predicted a_{ph} in nearshore waters, and solar radiation and SST were most important farther offshore over the hypoxic zone, indicating upwelled nutrient sources to phytoplankton. A multiple linear regression model performed well in resolving seasonal and interannual a_{ph} variability in model development years (2002–2004) (mean error of 18%, over all pixels and months) and in predicting shelf-wide a_{ph} patterns in 2005 (mean error of 32%). Our results strongly suggest that in recent years, stratification and vertical mixing, in addition to riverine [NO_3], play a primary role in regulating phytoplankton biomass over the hypoxic zone. As well, a springtime model experiment showed that a_{ph} over the hypoxic zone can differ by an average absolute 37% from its average scenario owing to changes solely in environmental variables other than NO_3 flux.

Citation: Green, R. E., and R. W. Gould Jr. (2008), A predictive model for satellite-derived phytoplankton absorption over the Louisiana shelf hypoxic zone: Effects of nutrients and physical forcing, *J. Geophys. Res.*, *113*, C06005, doi:10.1029/2007JC004594.

1. Introduction

[2] The Louisiana-Texas continental shelf is a highly dynamic river-dominated margin and the site of the 2nd largest zone of coastal hypoxia in the world. Increases in nitrate (NO_3) loading to the Mississippi River watershed during the last 50 years are considered responsible for an increase in summertime hypoxia in Louisiana-Texas shelf bottom waters [*Rabalais et al.*, 2002]. There is currently a national mandate to decrease the size of the hypoxic zone to 5000 km^2 by 2015, mostly by a 30% reduction in annual nitrogen flux into the Gulf of Mexico [*Mississippi River/Gulf of Mexico Watershed Nutrient Task Force*, 2001]. Hypoxic bottom waters (dissolved oxygen concentrations <2 mg L^{-1}) are a concern primarily because of the reduced catch of demersal fish, shrimp, and crabs in these waters [e.g., *Leming and Stuntz*, 1984], which otherwise represent one of the United States' most productive fisheries. High concentrations of dissolved NO_3 from the Mississippi River (>100 μM l^{-1} [*Dagg and Whitledge*, 1991]) support significant phytoplankton growth in the river plume [*Lohrenz et al.*, 1990, 1999]. When this primary production sinks from surface to bottom waters, it is consumed by aerobic bacteria and is considered an important factor leading to hypoxic conditions. Given the large areal extent of regional hypoxia (22,000 km^2 in midsummer 2002 [*Rabalais and Turner*, 2006]), a host of environmental factors determine primary production in surface waters over the hypoxic zone [e.g., *Lohrenz et al.*, 1999]. Assessing the mechanisms responsible for variability in phytoplankton growth on the shelf is requisite to a better understanding of hypoxia formation.

[3] On the basis of findings from in situ measurements, the interaction of circulation, light, and nutrient and freshwater inputs all act to regulate phytoplankton biomass and production on the Louisiana shelf. Seasonal variability in circulation and freshwater discharge from the Mississippi and Atchafalaya Rivers strongly influence the distribution of properties on the shelf. Maximum river discharge generally occurs in the spring (March–May) [*Dinnel and Wiseman*, 1986], and maximum retention of biomass and

[1]Ocean Optics Section, Naval Research Laboratory, Stennis Space Center, Mississippi, USA.

0148-0227/08/2007JC004594$09.00

nutrients on the shelf due to favorable winds and currents occurs from Fall through Spring [*Cochrane and Kelly*, 1986]. Conditions of both high discharge and favorable circulation have been associated with higher phytoplankton production and biomass on the shelf [e.g., *Chen et al.*, 2000]. As well, at a midshelf location between the Mississippi and Atchafalaya River mouths, primary production inferred from dissolved oxygen concentrations was positively correlated with river discharge (lagged by 2 months) over a six year period [*Justić et al.*, 1993]. Linkages between high concentrations of riverborne nutrients and productivity are the basis for management scenarios for regulating the size of summertime hypoxia. On the basis of measurements from several years, positive correlations were observed between primary production and NO_3 + nitrite (NO_2) concentrations near the Mississippi River delta [*Lohrenz et al.*, 1997]. Other biological and physical factors which cause variability in phytoplankton growth on the shelf include mixed layer irradiance, temperature, and salinity [*Lohrenz et al.*, 1990, 1997, 1999; *Chen et al.*, 2000], as well as phytoplankton species composition [*Redalje et al.*, 1994] and grazing [*Fahnenstiel et al.*, 1995]. While field measurements provide important insights into oceanographic processes, they are limited by the spatial and temporal scales of variability that they can capture.

[4] Satellite remote sensing has proved a powerful tool for studying oceanographic processes over large areal domains at relatively high spatial and temporal resolution. Imagery from the Coastal Zone Color Scanner (CZCS) ocean color satellite (1978–1985) provided the first climatological time series of phytoplankton concentration in the Gulf of Mexico [*Müller-Karger et al.*, 1991], showing high pigment concentrations during the winter and low concentrations during the summer. Seaward of the shelf, results from a combination of remote sensing observations and one-dimensional ecosystem modeling suggested that mixed layer depth was the single most important factor controlling seasonal pigment concentrations [*Walsh et al.*, 1989; *Müller-Karger et al.*, 1991]. Further inferences about phytoplankton in the open Gulf of Mexico were made using Sea-viewing Wide Field-of-view Sensor (SeaWiFS) ocean color data and a three-dimensional physical model [*Jolliff et al.*, 2008]. In addition to mixed layer depth, this analysis showed that mesoscale circulation significantly modulated bio-optical fields in the Gulf of Mexico, including phytoplankton pigments. Surface distributions of suspended particulate matter (SPM) have been studied in more coastal waters of the Gulf using satellite data. Analysis of Advanced Very High Resolution Radiometer (AVHRR) imagery (1989–1993) showed that river discharge and wind-forcing were the main factors driving seasonal variability in SPM distributions near the Mississippi River delta [*Walker*, 1996]. More recently, correlation analyses of SeaWiFS imagery (1997–2000) identified two distinct regions of SPM variability near the delta [*Salisbury et al.*, 2004]. Wind-driven variability of SPM was important in shallow areas, and this region was spatially separated from areas of high discharge-related variability.

[5] In recent years, significant effort has been devoted to the development of satellite ocean color algorithms that are valid for retrieving phytoplankton biomass in coastal regions. In Case 2 optical waters, the accurate retrieval of phytoplankton biomass from satellite imagery is complicated by the presence of multiple seawater constituents that affect remote sensing reflectance (R_{rs}). High concentrations of dissolved organic material and suspended sediments can result in the overestimate of chlorophyll concentration from satellites using empirical algorithms [e.g., *Darecki and Stramski*, 2004]. However, the use of in situ observations to regionally correct bio-optical algorithms can result in significantly improved satellite retrievals. For example, several studies have validated satellite retrievals with in situ data in coastal regions and have used the resulting chlorophyll algorithms to describe variability in phytoplankton biomass, including in Chesapeake Bay [*Harding et al.*, 2005] and Massachusetts Bay [*Hyde et al.*, 2007]. As well, accurate satellite retrievals of phytoplankton biomass in coastal waters is complicated by difficulties with atmospheric correction, which often result in satellite retrievals that are too low [e.g., *Siegel et al.*, 2000]. One successful technique for improving atmospheric correction in coastal regions applies an iterative method in which NIR water-leaving radiance is estimated from water leaving radiance at 670 nm [*Arnone et al.*, 1998; *Stumpf et al.*, 2003]; this NIR scheme improves retrievals of water-leaving radiances in coastal areas, has been implemented in the most recent (5th) global reprocessing effort of SeaWiFS at NASA, and was used in our image processing. As well, a new absorbing aerosol correction has been developed (which we have also applied during our image processing) that further improves satellite retrievals of phytoplankton biomass in Case 2 waters [*Ransibrahmanakul and Stumpf*, 2006]. Taken together, these advances in satellite image processing provide the unprecedented ability to better understand phytoplankton dynamics in the coastal zone.

[6] In the present study, our goal was to determine the main factors driving variability in satellite-derived phytoplankton absorption near the Mississippi River delta. Previous satellite-based time series analyses of phytoplankton biomass have focused mainly on waters seaward of the shelf in the Gulf of Mexico. We use extensive cruise data from shelf waters in the northern Gulf of Mexico to extend our understanding of phytoplankton dynamics to river-dominated Louisiana shelf waters. For a 3-year time period (2002–2004), we analyzed time series of SeaWiFS-derived phytoplankton absorption coefficients (a_{ph}) and a suite of potential environmental forcing mechanisms. We prefer a_{ph}, rather than chlorophyll concentration, as a proxy for phytoplankton biomass for two main reasons: (1) use of a_{ph} avoids methodological controversy in how chlorophyll is measured (i.e., fluorometric versus HPLC), and (2) as an optical property, a_{ph} should be more directly related to R_{rs}. In reality, a_{ph} is primarily a function of chlorophyll a and pheopigments, but also reflects physiological states related to photoadaptation [*Neori et al.*, 1984] and nutrient stress [*Heath et al.*, 1990]. First, we used correlation and stepwise regression analyses to determine the most important factors driving a_{ph} variability and their spatial patterns of influence. Second, a multiple linear regression model was developed for a_{ph}, and the prediction capabilities of this model were determined in application to SeaWiFS imagery for 2005. With relevance to mandated decreases in NO_3 loading to the Mississippi River watershed, we also applied the model to calculating variability in shelf phytoplankton distributions

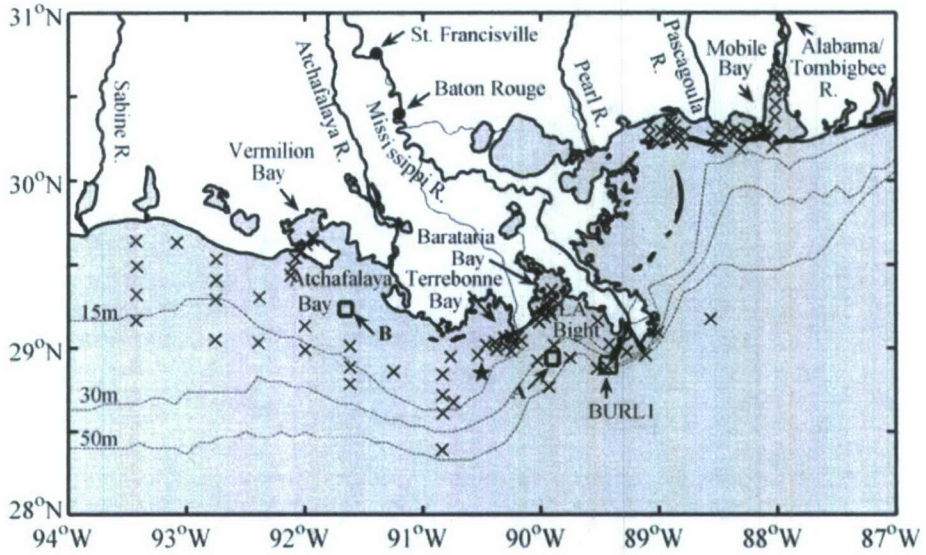

Figure 1. Map of study region in the northern Gulf of Mexico, including the Louisiana, Mississippi, and western Alabama coastlines. Locations of sample sites for all seven field experiments are indicated (crosses). Boxes A and B indicate regions in the Mississippi and Atchafalaya River plumes, respectively, where example average time series were calculated. The box at BURL1 indicates location of buoy wind measurements at Southwest Pass, which is the main outflow of the Mississippi River through the delta. Also, a site of long-term monitoring for hypoxia off Terrebonne Bay is indicated (station C6, star).

due to environmental variables other than NO_3 flux. This analysis should help explain observed changes in biomass that can't be accounted for by NO_3-flux variability alone.

2. Methods

2.1. Cruise Measurements

[7] Seven field experiments were conducted in northern Gulf of Mexico coastal waters of Louisiana, Mississippi and Alabama (Figure 1). Measurements were obtained during two cruises on the Louisiana shelf during 27 April to 1 May 2006 aboard the R/V *Pelican* and 6–11 September 2006 aboard the OSV *Bold*. Surface water samples were collected using a conductivity-temperature-depth profiler/rosette system equipped with sampling bottles. All samples were processed onboard ship within 2–3 h of sample collection. As well, two nearshore samplings in shallower waters of the Louisiana shelf were conducted as transects out of Vermilion, Terrebonne, and Barataria Bays (17–19 May and 17–19 July 2007). Three field experiments were also conducted off the Mississippi/Alabama coasts during 20–24 May 2002, 13 December 2005, and 6 February 2007. During these experiments, samples were collected on day trips and processed that evening or the next day onshore. Sample sites were generally located inside the 50 m isobath, with the majority of stations within the 15 m isobath (Figure 1).

[8] Absorption coefficients for particulate material (a_p) in surface water samples were measured spectrophotometrically. Particulate material was collected on GF/F filters (nominal pore size of 0.7 μm), and a_p was measured using an Analytical Spectral Devices (ASD) fiber optic-based spectrophotometer. Subsequent to the initial optical density measurements, filters were extracted for 20 min in hot methanol and reanalyzed to determine the residual particulate absorption by detritus (a_d) [*Kishino et al.*, 1985]. The absorption coefficient due to methanol-extractable phytoplankton pigments (a_{ph}) was estimated by difference between the initial and postextraction measurements ($a_p - a_d$). All measurements were relative to a blank filter saturated with milli-Q water, and the optical density (OD) at 850 nm for the blank was subtracted from each sample spectrum. A path length amplification (β) factor was used to correct optical density measurements for particle concentration and filter effects. The β factor was determined specifically for our ASD spectrophotometer during an experiment at Bigelow laboratory [*Mitchell et al.*, 2000], and was parameterized as

$$\beta(\lambda) = \left(0.258 + 1.153 \times OD_f(\lambda)\right)^{-1}, \quad (1)$$

where OD_f is the optical density of the filter pad. For field samples, duplicate measurements were generally not collected. However, for some coastal samples, heterogeneities were seen in the particulate material on the filter pad, and in these cases a second measurement was taken following rotation of the pad on the sample holder. A set of 122 phytoplankton absorption spectra were obtained in all.

2.2. Remote Sensing Imagery

[9] Local Area Coverage (LAC) SeaWiFS data of ~1 km resolution were collected, processed, and archived for the Gulf of Mexico region (80°W–98°W; 17°N–31°N). Imagery was acquired using a SeaSpace TeraScan satellite receiving system and processed with the Naval Research Laboratory's Automated Processing System (APS) [*Martinolich*, 2005]. APS Version 3.4 utilized atmospheric correction algorithms proscribed by NASA's fifth SeaWiFS

Table 1. Overview of Chemical and Physical Forcing Variables (2002–2004)

Variable	Range	Units	Source	Average $\|r\|$[a]	In Model[b]	% Pixels[c]
River Discharge (0 and 1 month lag)	6.2×10^3–2.8×10^4	$m^3\ s^{-1}$	USACE	0.26, 0.27	X, X	12, 9
River [SPM]	71–298	$mg\ L^{-1}$	USGS	0.20	X	5
River [NO_3] (0 and 1 month lag)	0.66–2.4	$mg\ L^{-1}$	USGS	0.28, 0.23	X, X	14, 6
River [PO_4]	0.030–0.091	$mg\ L^{-1}$	USGS	0.18		
River [SiO_3]	4.3–8.0	$mg\ L^{-1}$	USGS	0.16	X	6
Wind speed	3.7–8.2	$m\ s^{-1}$	NDBC	0.26	X	8
Wind u speed	−4.4–1.6	$m\ s^{-1}$	NDBC	0.18		
Wind v speed	−3.3–4.2	$m\ s^{-1}$	NDBC	0.21		
Wave height	0.47–1.6	m	LSU WAVCIS	0.15	X	4
Water height	0.13–0.52	m	LUMCON	0.22	X	7
Solar radiation	230–630	$\mu Ein\ m^{-2}\ s^{-1}$	LUMCON	0.27	X	8
Precipitation	0.28–18	mm	LUMCON	0.12		
Sea surface temperature (SST)	12–31	°C	IASNFS model	0.26	X	13
Current speed (SSS)	0–1.5	$m\ s^{-1}$	IASNFS model	0.22		
Current u speed (SSU)	−0.60–1.3	$m\ s^{-1}$	IASNFS model	0.18	X	4
Current v speed (SSV)	−1.0–1.3	$m\ s^{-1}$	IASNFS model	0.16	X	4

[a]Absolute correlation with a_{ph} time series as an average over the entire hypoxic zone (Figure 5).
[b]X denotes variables included in the final multivariate model.
[c]From stepwise analysis, the percent of pixels in which each variable was the most important predictor over the hypoxic zone.

reprocessing [*Arnone et al.*, 1998; *Stumpf et al.*, 2003]. The present atmospheric correction method used by APS improves estimates of bio-optical parameters in coastal regions by applying an iterative technique in which water-leaving radiance at 765 and 865 nm is estimated from water leaving radiance at 670 nm. An absorbing aerosol correction was also applied to improve underestimates of satellite-derived water reflectance [*Ransibrahmanakul and Stumpf*, 2006]. In our time series analyses, we used monthly composite imagery for 2002–2005 which were temporal averages of all valid pixels (e.g., cloud free) in each month.

[10] A relationship was developed between satellite-derived chlorophyll and in situ phytoplankton absorption measurements. We used a chlorophyll product which is automatically generated by APS, on the basis of the algorithm of *Stumpf et al.* [2000], hereafter referred to as "Stumpf chlorophyll." This algorithm is parameterized using a polynomial regression of the log-transformed ratio of remote sensing reflectance, R_{rs}, at 490 and 555 nm (*rat*). First, an initial chlorophyll value (C_i) in $\mu g\ L^{-1}$ is calculated as

$$C_i = 10^{-2.5 \times rat}. \quad (2)$$

The following algorithm is then applied which was developed specifically for coastal chlorophyll concentrations. This algorithm is a weighted transform which blends to the global OC2v2 chlorophyll algorithm in low-chlorophyll (offshore) waters:

$$\text{if } C_i \geq 0.5, \text{ then } C = C_i, \quad (3)$$

$$\text{if } 0.1 < C_i < 0.5, \text{ then}$$

$$C = 10^{\{\log_{10}(C_i) \times [\log_{10}(C_i)+1.0]+\log_{10}(C_{OC2}) \times (\log_{10}(0.5)-\log_{10}(C_i))\}/\log_{10}(5.0)},$$

$$\text{if } C_i \leq 0.1, \text{ then } C = C_{OC2} = 10^{\{a_1+rat \times [a_2+rat \times (a_3+rat \times a_4)]\}} + a_5.$$

The coefficients a_1 to a_5 are from the global chlorophyll algorithm (OC2v2) and equal 0.2974, −2.2429, 0.8358, −0.0077, and −0.0929 [*Maritorena and O'Reilly*, 2000]. It was not our intention to validate the Stumpf chlorophyll product for our study area, but rather to use satellite-derived values of this product to determine a relationship with our measurements of phytoplankton absorption at 443 nm. Satellite matchups with sample locations were taken from either the same day or, if not available, a day either side of sampling. Our derived relationship between satellite-derived Stumpf chlorophyll and measured a_{ph} (443) was then applied to all satellite imagery for the time series analyses to obtain satellite a_{ph} (443) imagery.

2.3. Time Series Analyses

[11] We compiled time series of numerous chemical and physical forcing variables near the Mississippi River delta (Table 1). The following environmental variables were chosen as those that could plausibly affect phytoplankton growth in surface waters. We used riverine discharge and NO_3 concentration ([NO_3]) as separate variables in our analysis to separate the physical effects of stratification from biological effects of eutrophication. Daily measurements of water discharge for the Mississippi River were obtained from the United States Army Corps of Engineers (USACE) for Tarbert Landing, Louisiana. Outflow from the Mississippi and Atchafalaya Rivers is highly in phase, reflecting efforts of the USACE to manage the discharge of the Mississippi River system so that ~2/3 of the discharge outflows via the bird-foot delta and the other 1/3 through the Atchafalaya (Figure 1). Concentrations of riverine NO_3 ([NO_3]), orthophosphate ([PO_4]), silicate ([SiO_3]), and SPM ([SPM]) were obtained from the United States Geological Survey (USGS) for St. Francisville and Baton Rouge, Louisiana (Figure 1); data were generally available bimonthly for each station. Daily values were interpolated from the USGS data and then monthly means were calculated. Two additional variables of riverine [NO_3] and discharge with a one month lag were also included in our analysis. Hourly measurements of wind speed and direction were obtained from the National Data Buoy Center (NDBC) for a station near the main Mississippi River outflow at Southwest Pass (BURL1; Figure 1). We analyzed wave height data from Louisiana State Univer-

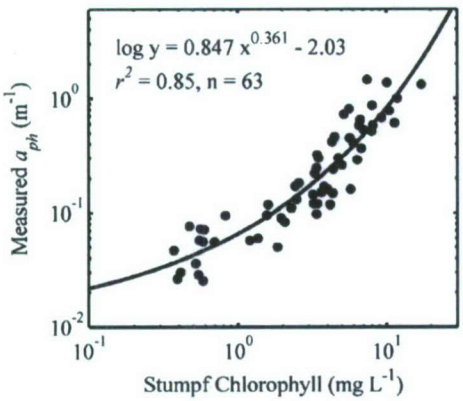

Figure 2. Algorithm for phytoplankton absorption (a_{ph}) at 443 nm as a function of satellite-derived chlorophyll. Stumpf chlorophyll was calculated from satellite-derived $R_{rs}(490)/R_{rs}(555)$ as described in section 2. Phytoplankton absorption values were determined from filter pad absorption measurements collected during seven cruises in the northern Gulf of Mexico. Note that the coefficient of determination (r^2 value) explains variance in log-transformed a_{ph}.

sity's (LSU's) Wave-Current-Surge Information System (WAVCIS) for Station 5 (−90°32′, 29°3.2′), which is located south of Terrebonne Bay. Several variables were obtained from the Louisiana Universities Marine Consortium (LUMCON) weather station, including solar radiation, precipitation, and water height.

[12] A physical circulation model provided sea surface temperature (SST), current magnitude (SSS), and current direction (SSU, SSV). We used the IntraAmericas Sea Nowcast/Forecast System (IASNFS) [*Ko et al.*, 2003] which consists of a 1/24° (5–6 km), 41-level, data-assimilating ocean model based on the Navy Coastal Ocean Model (NCOM) [*Martin*, 2000]. The IASNFS includes the Gulf of Mexico, the Caribbean Sea, the Straits of Florida, and part of the western North Atlantic Ocean. The ocean model continuously assimilates three-dimensional ocean temperature/salinity analyses produced by a statistical data analysis model, the Modular Ocean Data Assimilation System (MODAS) [*Carnes et al.*, 1996]. Real-time satellite altimeter sea surface height anomaly data, as well as AVHRR SST data are assimilated into the model. Surface forcing is provided by surface wind stress, heat fluxes, solar radiation, air pressure, and river discharge (monthly climatology) from 53 rivers. Rivers are prescribed by river temperature (monthly climatology), salinity (fresh water), and discharge as a function of depth. The open boundary conditions are provided by barotropic tidal forcing and the Navy's global NCOM model [*Ko et al.*, 2007]. We define currents and winds in the u (zonal) and v (meridional) directions, where positive u is to the east and positive v is to the north. For our analysis, we interpolated SST and currents to the higher resolution of the SeaWiFS imagery in a region encompassing the Louisiana shelf (latitudes 28.4°N to 30°N, longitudes 89°W to 94°W). Mean monthly values were calculated for all environmental variables.

[13] Correlation and regression analyses were performed to analyze the impacts of the different forcing variables on driving mean monthly optical variability. In the case of point measurements, such as river discharge and wind speed, the same physical time series was assumed at all image pixels. In contrast, a unique physical time series at each image pixel was used for IASNFS model results. Spikes were removed from satellite-derived $a_{ph}(443)$ time series by discarding points that were more than five times the mean at each pixel over the 3 year study period (2002–2004). As a first step, correlation analyses were performed between mean monthly satellite-derived $a_{ph}(443)$ time series for 2002–2004 and each forcing variable. Next, we used stepwise multiple linear regression analysis to determine the importance of the different variables in determining a_{ph} variability. A forward stepwise procedure was used in which the most statistically significant term (the one with the lowest p value for $p < 0.05$) is added into the model at each step, until there are no statistically significant terms left to include. A common problem with multiple regression analysis is multicollinearity of the input variables, a point which we will further discuss. On the basis of the stepwise analysis, several variables were identified as least important and were removed from our final multivariate model.

[14] Using the 2002–2004 data sets, a multiple linear regression model for a_{ph} was developed at each pixel, such that forcing variables had different model weightings depending on location. The resulting model was then applied to predicting a_{ph} for several different scenarios. Mean monthly environmental variables for 2005 were input to the model to determine how well temporal and spatial variability in a_{ph} could be predicted for a year that was not included in model development. As well, we performed an experiment with the model to see how much a_{ph} could change in spring (April–June) 2002–2004 on the basis of natural variability in all environmental variables, except nitrate flux (riverine $[NO_3] \times$ discharge). For this experiment, a maximum and minimum a_{ph} scenario were modeled using the measured limits of all springtime environmental variables, while both riverine $[NO_3]$ and discharge were held constant at their average values for this time period. Decreases in nitrogen flux from the Mississippi River to the Gulf of Mexico have been mandated in order to reduce the size of summertime hypoxia [*Mississippi River/Gulf of Mexico Watershed Nutrient Task Force*, 2001]. As riverine NO_3 flux is reduced, certainly other environmental factors will cause some variability in phytoplankton biomass on the shelf and the size of hypoxia. Thus, we wanted to explore how much these other sources of variability could affect a_{ph}. The experiment was performed for the spring, a period during which in situ phytoplankton growth in surface waters is considered important in the development of regional hypoxia. We performed all time series data analyses using the MATLAB software package (The MathWorks).

3. Results

3.1. Algorithm Development

[15] We developed a regional algorithm for phytoplankton absorption at 443 nm based on satellite-derived remote sensing reflectance for the northern Gulf of Mexico (Figure 2). Measurements of $a_{ph}(443)$ on the Louisiana

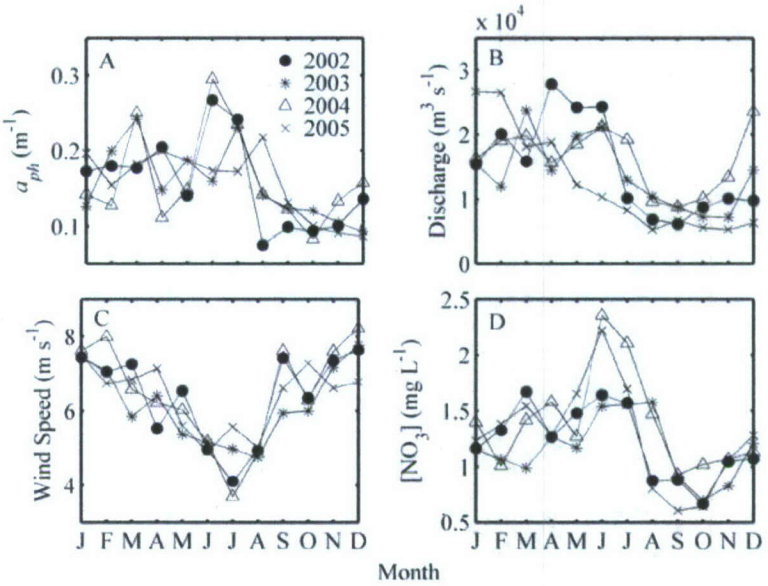

Figure 3. For 2002–2005, time series of (a) satellite-derived a_{ph} (443), (b) Mississippi River discharge, (c) wind speed, and (d) riverine [NO_3]. The a_{ph} time series presented here are an average over Box A in the Louisiana Bight (Figure 1). The first 3 years (2002–2004) were used to develop the optical model, which was subsequently applied to 2005 data to predict a_{ph} for that year.

shelf from all four field experiments ranged from 0.02 to 2.9 m^{-1}. Peak values were measured in Barataria Bay during nearshore sampling in May and July, 2007. Of the 122 measured a_{ph}(443) values, there were only 63 matchups with satellite imagery owing to clouds over the sample site. There was substantial variability in measured a_{ph}(443) for the same value of satellite-derived chlorophyll concentration (Figure 2), and this variability was even within a single field experiment. This variability in a_{ph}(443) averaged ~2.5-fold, similar to previous observations in these waters [*D'Sa et al.*, 2006]. A good fit was obtained between satellite-derived Stumpf chlorophyll and log-transformed values of measured a_{ph}(443) using a power function (r^2 = 0.85; RMSE = 0.18). This relationship was used to calculate the satellite-derived a_{ph}(443) product used in the following time series analyses.

3.2. Physical Time Series

[16] For 2002–2005, phytoplankton absorption peaked from late winter to summer (March–August) on the Louisiana shelf, with significant spatial and interannual variability observed in peak magnitude and timing. Highest a_{ph} values were usually associated with the Mississippi and Atchafalaya River outflows, though locally high values were also observed outside of Barataria Bay and near the Sabine River outflow. To exemplify temporal trends, we analyzed a_{ph} in two different regions of the shelf: the Louisiana (LA) Bight in the Mississippi River plume (Box A; Figure 1) and the Atchafalaya River plume (Box B). Values of a_{ph} in Boxes A and B ranged from 0.08 to 0.30 m^{-1} and 0.17 to 0.79 m^{-1}, such that a_{ph} in the Atchafalaya plume box was ~2 times higher than in the Mississippi plume box. Differences in peak timing were also observed between the two regions. Whereas a_{ph} in the Atchafalaya plume always peaked in July (not shown), maxima in the Mississippi plume were observed from March through August, depending on the year (Figure 3a). As well, interannual and spatial variability was observed in whether a_{ph} had one or two annual peaks. A notable exception to peak timing was occasionally observed in the southernmost region of the hypoxic zone, south of 29°N latitude (extent of hypoxic zone shown in Figure 5). In this region, the influence of offshore waters, most likely in the form of upwelled nutrients, occasionally caused a_{ph} to peak in winter (December–January).

[17] Most environmental forcing variables demonstrated some degree of seasonal trend during the period of our study. As expected, highest values were observed for river discharge in winter to spring (Figure 3b), for wind speed in winter (Figure 3c), and for riverine [NO_3] in spring to summer (Figure 3d). Springtime maxima were also generally observed in solar radiation, precipitation, and wave height, and summertime maxima were observed in [PO_4] and water height and for SST in the Louisiana Bight. Wintertime peaks were observed in both [SPM] and [SiO_3]. Both wind and current u speed (SSU in LA Bight) were largest to the west in winter, and wind and current v speed (SSV in LA Bight) to the north in spring. Throughout much of the year, winds and Ekman transport caused circulation to flow westward over the Louisiana shelf (e.g., Figure 4) [*Cochrane and Kelly*, 1986]. However, between November and February, this general pattern was periodically altered by N or NW winds associated with the passage of continental air masses causing offshore circulation over the Louisiana shelf. Also, in July offshore flow was always observed owing to periods of W winds.

[18] A correlation matrix was computed for all time series (Table 2). In the Mississippi River plume (Figure 1, Box A), a_{ph} was significantly correlated with five forcing variables, including (in order of importance) discharge (r = 0.59), [NO_3] (r = 0.51), lagged discharge (r = 0.49), wind speed

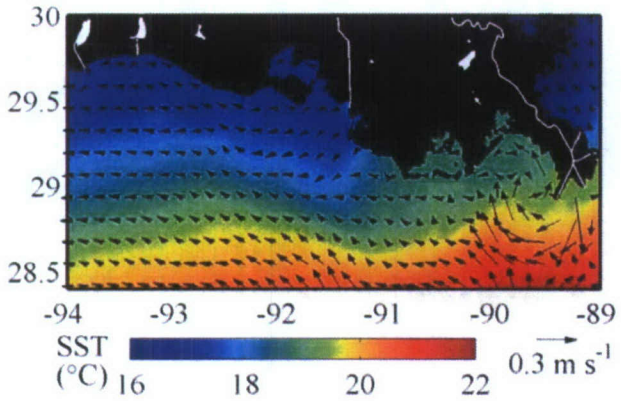

Figure 4. Example IntraAmericas Sea Nowcast/Forecast System (IASNFS) circulation model fields for sea surface temperature (SST), current speed (SSS), and current direction as a mean for March 2002. This example is representative of mean westward flow over the Louisiana shelf during much of the year.

(r = −0.33), and solar radiation (r = 0.33). Of the 171 possible correlations between the 18 forcing variables, 33% were considered significant, with an absolute r value > 0.33 (two-tailed test, α = 0.05). Particularly high correlations ($|r|$ > 0.70) were observed between [NO_3] and lagged discharge, [PO_4] and SST, wind speed and SST, and SSS and SSU. In contrast to the Mississippi River plume, a_{ph} in the Atchafalaya River plume (Figure 1, Box B) was most highly correlated with [NO_3] (r = 0.59), followed by wind speed (r = −0.55) (data not shown).

3.3. Correlation Analyses

[19] We first performed simple correlation analyses between time series of a_{ph} and each environmental forcing variable for 2002–2004. An average correlation coefficient for each variable was calculated over the hypoxic zone (Table 1 and Figure 5). This zone is here defined as the region from the coast to the maximum seaward extent of hypoxic waters in summer based on measurements from 1985 to 2002 [*Turner et al.*, 2006]. Average correlations showed that six variables were most important in determining a_{ph} variability ($|r| \geq 0.26$), including river discharge with 0 and 1 month lags, riverine [NO_3] (0 lag), wind speed, SST, and solar radiation (Table 1 and Figure 5). Average correlations were generally low, because values were computed over the entire hypoxic zone (Table 1). However, much higher values (up to 0.85) were observed in some regions (Figure 5). In nearshore waters, a_{ph} was positively correlated with all six most important variables, except wind speed with which it was negatively correlated. In offshore waters, but still over the hypoxic zone, a_{ph} was negatively correlated with SST and solar radiation. Thus, two different modes of forcing were observed for SST and solar radiation depending on cross-shelf location.

[20] Although of less overall importance, the other environmental variables in our analysis were significantly correlated ($|r|$ > 0.33) with a_{ph} somewhere in our region of interest. For example, riverine [NO_3] lagged by 1 month roughly showed correlation patterns (not shown) similar to [NO_3] (0 lag), though of slightly lower magnitude (Table 1). Higher wind and current speeds toward the east were positively and significantly correlated with a_{ph} in the Atchafalaya plume. This corresponds to our previous observation of maximum a_{ph} occurring in the Atchafalaya plume in July, a month when currents were always eastward. Higher wind and current speeds toward the north were positively and significantly correlated with a_{ph} in the Louisiana Bight, reflecting the increased impact of the Mississippi River plume under these conditions. Water height showed significant, but negative, correlations with a_{ph} in a region south of Atchafalaya and Terrebonne Bays between the coast and 50 m isobath. These findings emphasize the high degree of spatial variability observed in the environmental factors which drive a_{ph} in a region as large as the Louisiana shelf.

Table 2. Correlation Matrix for a_{ph} and Forcing Variables in the Louisiana Bight (2002–2004)[a]

	a_{ph}	Dis	DisL	SPM	[NO_3]	[NO_3]L	[PO_4]	[SiO_3]	Wnds	Wndu	Wndv	WavH	WatH	Rad	Prec	SST	SSS	SSU	SSV
a_{ph}	1.00																		
Dis	**0.59**	1.00																	
DisL	**0.49**	**0.53**	1.00																
SPM	0.32	**0.51**	0.21	1.00															
[NO_3]	**0.51**	**0.48**	**0.70**	0.15	1.00														
[NO_3]L	0.27	0.18	**0.48**	−0.17	**0.52**	1.00													
[PO_4]	−0.14	**−0.42**	−0.11	**−0.52**	0.14	0.29	1.00												
[SiO_3]	0.05	0.01	−0.09	0.01	0.19	−0.04	**0.40**	1.00											
Wnds	**−0.33**	−0.09	**−0.42**	**0.37**	**−0.50**	**−0.66**	**−0.39**	0.18	1.00										
Wndu	0.17	0.16	0.17	−0.15	**0.44**	0.27	0.06	0.17	**−0.41**	1.00									
Wndv	0.19	0.19	**0.51**	0.00	**0.46**	0.25	0.18	−0.20	**−0.58**	0.04	1.00								
WavH	0.07	0.29	0.08	**0.44**	0.05	**−0.36**	−0.26	−0.09	**0.43**	−0.24	0.19	1.00							
WatH	−0.10	−0.25	−0.20	−0.29	−0.13	0.20	**0.49**	−0.14	**−0.33**	−0.13	0.12	−0.05	1.00						
Rad	**0.33**	0.28	**0.61**	−0.08	**0.51**	**0.58**	0.21	**−0.34**	**−0.68**	−0.01	**0.68**	0.02	**0.36**	1.00					
Prec	−0.20	−0.06	−0.09	−0.25	0.01	−0.07	0.30	0.08	−0.20	0.10	**0.35**	−0.01	0.25	−0.06	1.00				
SST	−0.03	−0.27	0.10	**−0.57**	0.23	**0.48**	**0.83**	0.05	**−0.73**	0.13	**0.50**	−0.25	**0.64**	**0.58**	**0.34**	1.00			
SSS	0.19	**0.33**	0.10	0.29	−0.07	0.14	−0.15	−0.18	0.09	**−0.58**	0.12	0.32	0.13	**0.39**	−0.21	−0.05	1.00		
SSU	0.03	−0.14	0.16	−0.23	**0.37**	0.05	0.20	0.17	−0.29	**0.65**	0.15	−0.26	−0.08	−0.11	0.20	0.17	**−0.87**	1.00	
SSV	0.29	**0.35**	0.20	0.14	0.26	0.30	−0.05	−0.31	**−0.33**	−0.23	**0.34**	0.20	0.12	**0.49**	−0.05	0.14	**0.55**	−0.28	1.00

[a]Correlations in this table for a_{ph}, SST, SSS, SSU, and SSV are averaged over Box A (Figure 1). Absolute values greater than the critical value of 0.33 (α = 0.05) are in bold. N = 36. Variables: Dis, Mississippi River discharge; DisL, 1 month lagged river discharge; [NO_3]L, 1 month lagged [NO_3]; Wnds, wind speed; Wndu, wind u speed; Wndv, wind v speed; WavH, wave height; WatH, water height; Rad, solar radiation; Prec, precipitation.

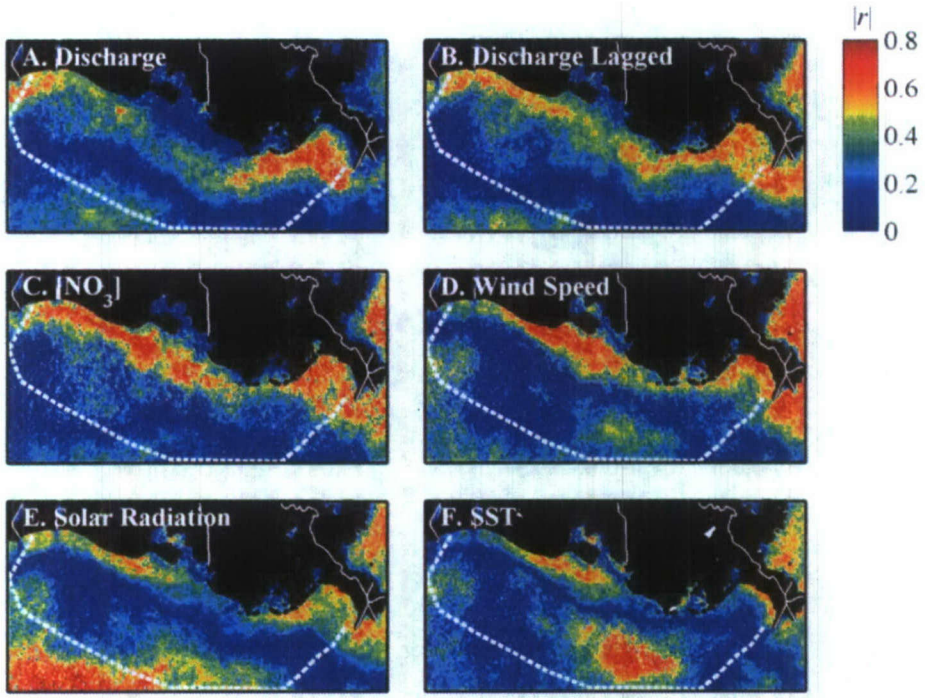

Figure 5. For mean monthly time series (2002–2004), absolute correlation of satellite-derived a_{ph} (443) with (a) Mississippi River discharge, (b) river discharge with 1 month lag, (c) riverine [NO_3], (d) wind speed, (e) solar radiation, and (f) SST. The maximum seaward extent of the hypoxic zone is indicated (dashed line) [*Turner et al.*, 2006].

3.4. Phytoplankton Absorption Model

[21] Stepwise multiple linear regression analysis was used to determine the importance of the various environmental variables in determining a_{ph} on the shelf. Only significant variables ($p < 0.05$) were retained in the model (see section 2). We calculated the importance of each variable based on the number of pixels in which it was included in the stepwise model over the hypoxic zone. The six most important variables were [NO_3] (0 lag), discharge with 0 and 1 month lags, SST, solar radiation, and wind speed: the same variables identified in the correlation analyses. At each pixel, we determined which of these variables was the best predictor of a_{ph}, and we observed coherent spatial patterns across the shelf (Figure 6). Discharge and [NO_3] (including lagged variables) were the most important predictors of a_{ph} over the hypoxic zone and were approximately equal in importance. Discharge was spatially the best predictor along a band stretching from the Mississippi River delta to the Sabine River. Nitrate concentration and wind magnitude tended to be the best predictors of a_{ph} in shallow, nearshore waters, whereas solar radiation and SST were the best predictors farther offshore. Although [NO_3] appears to be important in some waters farther offshore (Figure 6), in these regions the relationship between [NO_3] and a_{ph} was generally not significant ($p > 0.05$). On the basis of the stepwise analysis, we also found that certain parameters were not important to include in the a_{ph} model, including wind u and v magnitude, [PO_4], precipitation, and current speed. These five parameters were least often included in the stepwise model and generally did not show coherent spatial patterns in their model inclusion; they were removed from the following analyses.

[22] A multiple linear regression model was developed for phytoplankton absorption at each pixel using the remaining environmental variables (Table 1). Thus, different model weightings were assigned to forcing variables depending on location. We then applied the model to the environmental data to create monthly a_{ph} distribution maps for comparison with the satellite monthly composite a_{ph} imagery. For mean monthly time series (2002–2004), the average correlation coefficient (r) between modeled and satellite-derived a_{ph} was 0.82 over our region of interest with all variables included. The five least important parameters (wind u and v magnitude, [PO_4], precipitation, and current speed) were removed to develop the most parsimonious model. The resulting multiple regression model performed well, with modeled and satellite-derived a_{ph} time series that were significantly correlated at all pixels and with an average r of 0.75. The main seasonal and interannual features in a_{ph} were generally resolved (e.g., Figures 7 and 8). However, there were occasional differences between satellite and modeled a_{ph}, such as in the westward orientation of the Atchafalaya River plume in October 2002 (Figures 7g and 7h) and in the seaward extent of the Mississippi River plume in April 2003 (Figures 8c and 8d). The overall difference between satellite and modeled a_{ph} was 18%, averaged over all months and pixels.

[23] The model performed well in resolving seasonal and interannual monthly differences in a_{ph} for the years used in model development. In the Louisiana Bight (Box A, Figure 1), seasonal maxima in satellite-derived a_{ph} for

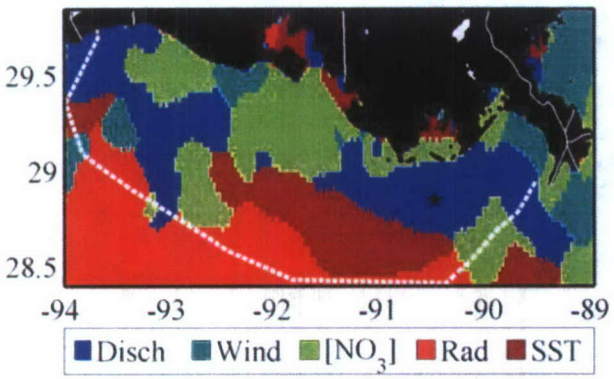

Figure 6. For mean monthly time series (2002–2004), regions where each variable listed was the most important in driving $a_{ph}(443)$. This was determined from stepwise multiple linear regression analysis for the most important variables overall: discharge (Disch), wind, $[NO_3]$, solar radiation (Rad), and SST. In this figure, discharge and $[NO_3]$ include both the 0 and 1 month lagged variables. A smoothed image for eased interpretation was produced by repeatedly passing a 3 × 3 window over the image and assigning the most likely value to the center pixel. The seaward extent of the hypoxic zone is indicated (dashed line), as is a site of long-term hypoxia monitoring (station C6, star).

2002–2004 were observed from March to July and minima from August to December (Figure 3a). These seasonal trends were also seen in the modeled a_{ph} distributions (e.g., Figure 7). For example, in 2002, a_{ph} in the Mississippi and Atchafalaya plumes (Boxes A and B) were both higher in July than in October (Figures 7e–7h). We adjusted values of the different forcing variables to determine which environmental variables were primarily responsible for observed differences in a_{ph}. In the Mississippi plume, lower wind magnitude in July 2002 (Figure 3c) was one of the primary causes of higher a_{ph} than in October 2002. In contrast, in the Atchafalaya plume, higher $[NO_3]$ in July was the main cause of higher a_{ph} than in October. In addition to seasonal patterns, interannual monthly differences in a_{ph} were also represented by model results (e.g., Figure 8). For example, compared to 2003 and 2004, spatial patterns in April 2002 were characterized by a_{ph} that was higher in the Mississippi plume (Box A) and lower in the Atchafalaya plume (Box B) in both satellite and modeled a_{ph}. In the Mississippi plume, lower river discharge and higher wind magnitude in both 2003 and 2004 (Figures 3b and 3c) noticeably decreased a_{ph} compared to 2002. In contrast, in the Atchafalaya plume, higher SSV in 2003 and higher $[NO_3]$ in 2004 (Figure 3d) were the primary reasons for higher a_{ph} than in 2002.

3.5. Model Predictions

[24] Our ultimate goal was to develop a model for predicting phytoplankton absorption at monthly timescales, in a year that was independent of model development. To this end, we applied the regression model to 2005 environmental data. Application of the model to 2005 was a good test of prediction capabilities, as river discharge (and certain other environmental variables) was often outside the ranges that went into model development (Figures 3b–3d). These instances often lead to modeled values of a_{ph} which were negative. To correct for this, if an environmental variable in 2005 was higher (or lower) than the range for that variable in model development, we substituted it with the maximum (or minimum) value for that particular month from 2002 to 2004. The resulting model for 2005 lead to a mean error between satellite and modeled a_{ph} of 32% over all pixels and months, which, as expected, was higher than the 18% error we observed for 2002–2004. For comparison, the average error between satellite imagery and a_{ph} climatology (1998–2007) was also calculated. This error with climatology was slightly lower (27%) than from the model (32%), but the model provides the additional benefit of elucidating the factors driving optical variability, which cannot be gained from the climatology alone. Expected patterns in shelf-wide a_{ph} were generally reproduced by our model in 2005 (e.g., Figure 9). For example, the model helped explain higher values of satellite-derived a_{ph} on the Louisiana shelf early in 2005, compared to late in the year. In the Mississippi plume (Box A), we identified higher river discharge and $[SiO_3]$ in January 2005 (e.g., Figure 3b) as important drivers of the higher a_{ph} observed in January compared to December (Figure 3a). In the Atchafalaya River plume (Box B), higher lagged river discharge in January 2005 was primarily responsible for higher a_{ph} compared to December 2005. As well, mean monthly time series of satellite-derived and model-predicted a_{ph} compared well in 2005. For example, both satellite and modeled a_{ph} peaked in spring to early summer in the Mississippi River plume (Box A; Figure 10a), in comparison to midsummer peaks in the Atchafalaya River plume (Box B; Figure 10b).

[25] We also did an experiment with the model to determine the impact environmental factors other than NO_3 flux have on the distribution and magnitude of a_{ph} on the Louisiana shelf. Environmental data were changed within the natural variability observed for spring (April–June) 2002–2004, while NO_3 flux (riverine $[NO_3]$ × discharge) was held constant at its average value for that period. Previously, we considered the separate effects of riverine discharge and nutrient concentration. However, in this experiment, we consider the two together as NO_3 flux, because this is the quantity specified by mandated nutrient reductions [*Mississippi River/Gulf of Mexico Watershed Nutrient Task Force*, 2001]. A springtime scenario using average environmental data (Figure 11a) was compared to maximum and minimum a_{ph} scenarios (Figures 11b and 11c). These scenarios were modeled using the limits of all springtime environmental variables, except NO_3 flux. On the basis of our model for 2002–2004, the results suggested that springtime a_{ph} over the hypoxic zone could vary by an average absolute difference of 37% from its average a_{ph} scenario owing to changes in environmental variables other than NO_3 flux. The three most important nonflux variables causing variability in the spring were $[SiO_3]$, SST, and solar radiation, which contributed 25% of the 37% change in a_{ph}. Much higher variations in a_{ph} were observed in specific regions of the shelf. For example, in some regions of the Louisiana Bight (Figure 1), a_{ph} varied by an average absolute difference of ~100% from its average a_{ph} scenario. In a second experiment, riverine $[NO_3]$ (versus flux) was held

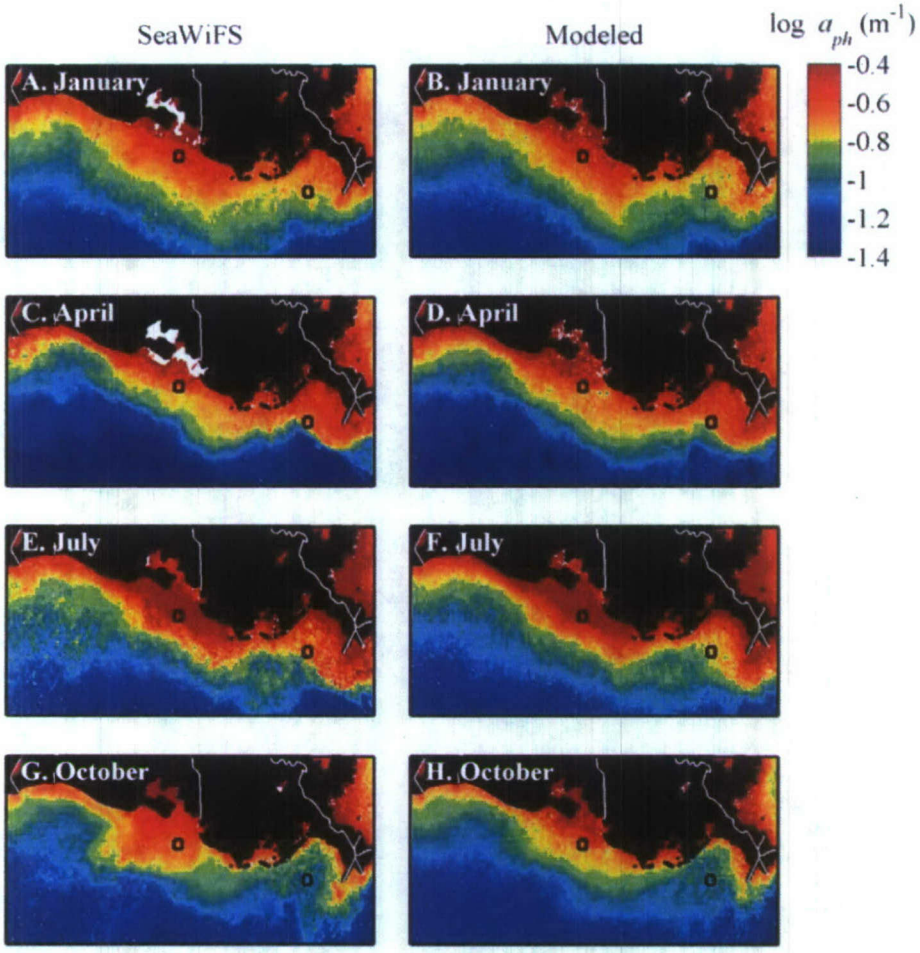

Figure 7. For 2002, multiple linear regression model performance comparing satellite-derived a_{ph} (left-hand column) and modeled a_{ph} (right-hand column) in an example from each season. On each plot, the location of boxes A and B (Figure 1) in the Mississippi and Atchafalaya River plumes, respectively, is indicated. White pixels in SeaWiFS imagery represent algorithm failures (i.e., chlorophyll retrieval failure, so subsequent a_{ph} calculation also failed).

constant, and average springtime a_{ph} over the hypoxic zone varied by an average absolute difference of 42% from its average a_{ph} scenario owing to changes in all other environmental variables (including discharge in this case).

4. Discussion

[26] Our understanding of phytoplankton dynamics from the regression model is only as good as the accuracy of satellite retrievals in coastal regions. In coastal waters, the accurate retrieval of phytoplankton absorption is complicated by high concentrations of dissolved organic material and suspended sediments, components which may sometimes covary with phytoplankton concentrations. Satellite algorithm errors are also caused by differences in measurement times between in situ collection and satellite overpasses [e.g., *Chang and Gould*, 2006]. For example, our absorption measurements were made at various times of the day, whereas the SeaWiFS overpass occurs near local noon. As well, if the measurement day was cloudy, we allowed satellite matchups from a day either side of our actual measurements. Another issue in coastal regions is that high spatial variability can occur at smaller spatial scales than are resolved by the satellite [*Yuan et al.*, 2005], further contributing to errors in satellite-based algorithms. Despite potential problems, a great deal of effort is now focused on advancing satellite applications to continental shelves, given that these are regions with the world's highest oceanic productivity and which are increasingly impacted by human activities. To obtain the best satellite retrievals possible, we have used a large in situ data set for satellite validation and have applied the most up-to-date atmospheric and absorbing aerosol corrections.

[27] We developed a multivariate model for phytoplankton absorption on the Louisiana shelf from a suite of chemical and physical forcing mechanisms, based on 3 years of data. The final multiple regression model included 13 environmental variables (Table 1) and performed well in determining temporal and spatial variability in a_{ph} for 2002–2004 (average r = 0.76). The six most important variables, as determined from stepwise analysis, were river discharge with no lag and one month lag, riverine

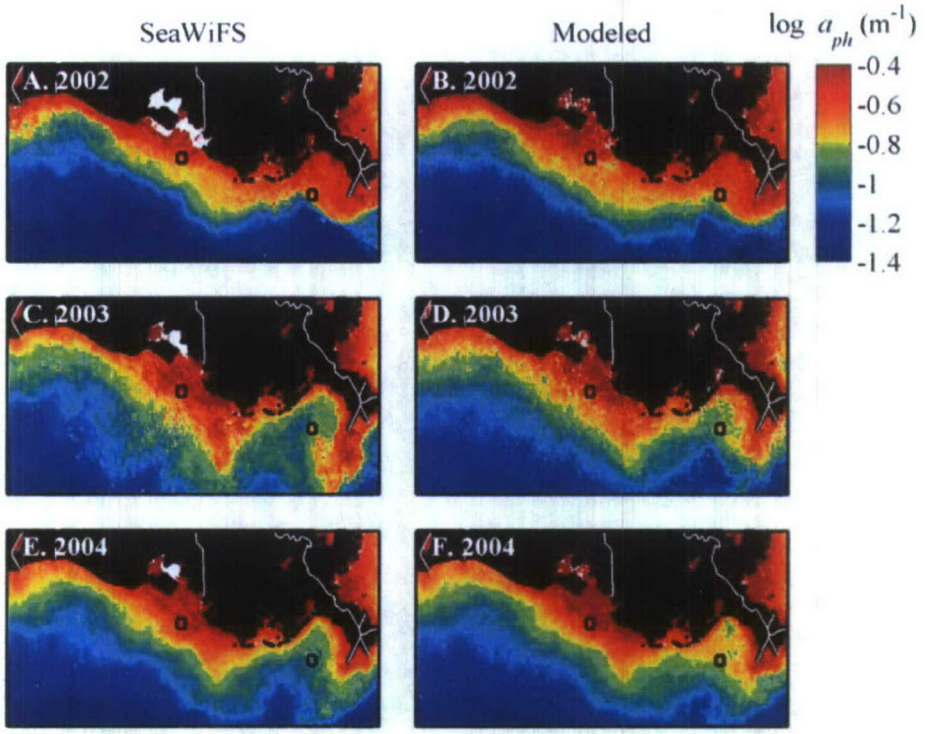

Figure 8. For April, multiple linear regression model performance comparing satellite-derived a_{ph} (left-hand column) and modeled a_{ph} (right-hand column) in each year for which the model was developed (2002–2004). On each plot, the location of boxes A and B (Figure 1) in the Mississippi and Atchafalaya River plumes, respectively, is indicated.

$[NO_3]$ (no lag), wind magnitude, SST, and solar radiation. Our multivariate model is a statistical model which allows for the determination of relationships between variables. A statistical model does not necessarily represent the underlying causal mechanisms in the way that a mechanistic model would. In addition, it will only describe temporal variability for the years of our study (2002–2004) and on scales comparable to the data scales (monthly in this case; e.g., tidal effects would be difficult to distinguish). For example, higher prediction errors would be observed in years with significantly different forcing variables than were encompassed by the model, as evidenced in our predictions for 2005, a year with river discharge outside the extremes of model parameterization (Figure 3b). However, mechanistic models of phytoplankton growth in river-dominated ocean margins are still in relatively early stages of development, in terms of spatial and temporal resolution [e.g., *Green et al.*, 2008]. In our current statistical analysis, we interpret relationships between a_{ph} and environmental variables carefully, since one environmental variable may be cross-correlated with another variable in our study (Table 2), or there may be important controlling variables that were not considered here.

4.1. Physical Factors Controlling Phytoplankton

[28] Freshwater discharge from the Mississippi River was one of the most important predictors of phytoplankton absorption over the hypoxic zone. We emphasize that this discharge is related to buoyancy flux and stratification effects, and not with nutrients in the discharge, because both variables are included separately in our analysis. For recent years, our work strongly supports "discharge driven" as one of the best descriptors of shelf phytoplankton biomass (Figures 5a and 6), as proposed by *Biggs and Sanchez* [1997]. In previous work, analysis of suspended particulate matter (SPM) distributions also showed that river discharge was the most important factor determining the Mississippi River plume's westward extent on the shelf [*Walker*, 1996]. Only two analyses of long-term in situ data sets have studied correlations between Mississippi River discharge and shelf phytoplankton growth. Using data from midsummer, hypoxia monitoring cruises (1985–1991), a significant positive correlation was demonstrated between primary production and river discharge lagged by one month (r = 0.84) at station C6, a site located between the Mississippi and Atchafalaya River outflows [*Justić et al.*, 1993]. This result agrees with our findings, with station C6 located centrally in the discharge-dominated region of our study (Figure 6). In a second study, in situ primary productivity data from several years (1988–1994) was averaged over large spatial areas of the shelf [*Lohrenz et al.*, 1997]. These average data sets showed no significant correlations with discharge. However, the contrasting result with our study is likely a difference in spatial representation, with over half of Lohrenz et al.'s measurements collected outside of the discharge-dominated regions delineated in our study. We propose two physical mechanisms by which discharge could increase phytoplankton biomass on the shelf: (1) physical advection of fresh, high-biomass waters farther

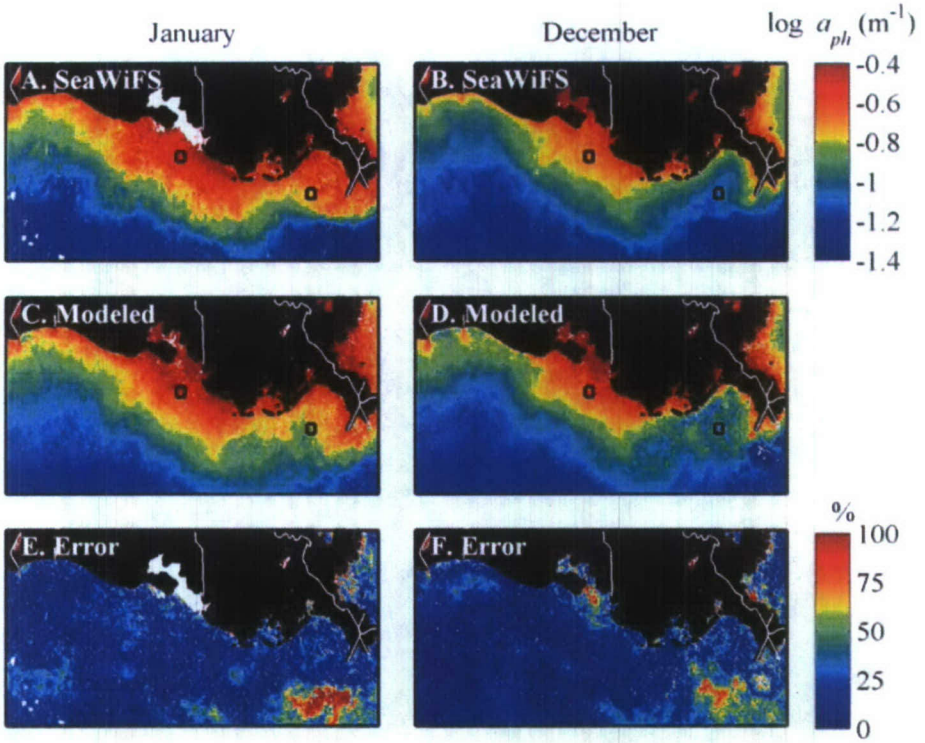

Figure 9. For 2005, comparison of (top) satellite-derived a_{ph} and (middle) model-predicted a_{ph}. (bottom) The % error between SeaWiFS and modeled images was calculated using the absolute value of the difference and referenced to SeaWiFS. These months exemplify application of the model to predicting a_{ph} in a year that was not included in model development. White pixels in modeled fields represent regions of model failure (i.e., negative values of modeled a_{ph}).

down-shelf from river mouths (at mid to high salinities), and (2) increased water column stratification leading to reduced mixing and subsequently, reduced light limitation of growth (at low salinities). On the basis of previous observations, light limitation of phytoplankton growth in the Mississippi River plume is probably mainly a factor at lower salinities [e.g., *Lohrenz et al.*, 1999]. In the Louisiana Bight, spring/summer maxima in Mississippi River [NO_3] should reinforce the positive impact of discharge on phytoplankton biomass (Table 2).

[29] Wind speed was also an important contributor to a_{ph} variability on the Louisiana shelf. The wind-dominated region was predominantly in shallow areas, and spatially distinct from that of the discharge-dominated region which was slightly farther offshore (Figures 5 and 6). Similarly, a time series analysis of satellite-derived SPM concentrations demonstrated spatially distinct zones of discharge- and wind-driven forcing on the shelf [*Salisbury et al.*, 2004]. Further comparison with this study exemplifies differences between the physical forcing of phytoplankton cells that are actively growing and generally less dense, in comparison to mineral and detrital particles. For example, in our study of phytoplankton, the discharge-dominated region extended farther west from the Mississippi River mouth, most likely because riverborne SPM sinks quickly from surface waters [e.g., *Corbett et al.*, 2004]. In addition, the size of the wind-dominated region was much larger in the SPM study. *Salisbury et al.* [2004] hypothesized that positive wind-SPM correlations were largely an expression of wind-driven processes of sediment resuspension and transport of suspended particles from shallower to deeper waters. In contrast, we observed a negative correlation between wind speed and a_{ph}. We hypothesize that increased wind speed causes light limitation of phytoplankton growth either due to a deeper mixed layer or resuspension of light-attenuating materials into the water column. In fact, changes in measured a_{ph} in shallow regions of the shelf have been linked to wind events. Following passage of a cold front with increased wind speeds, a_{ph} in a nearshore region of the Louisiana Bight decreased by twofold in March 2002, while absorption by CDOM increased [*D'Sa et al.*, 2006]. This change in a_{ph} may have been caused by either the change in wind speed or wind direction with frontal passage. Because higher wind speeds were correlated with more southerly winds in our study (Table 1), the two factors may act together to decrease a_{ph} in shallow waters.

[30] The importance of sea surface temperature and solar radiation in the southern region of the hypoxic zone indicates a contribution from upwelled nutrients to phytoplankton farther offshore on the Louisiana shelf. Whereas nutrient concentrations are higher in low-salinity shelf waters, farther offshore on the shelf nutrient concentrations are often negligible, especially in Fall and Winter [e.g., *Lohrenz et al.*, 1999; *Chen et al.*, 2000]. In our study, both solar radiation and SST varied seasonally with minima in winter. In contrast, in the southern region of the hypoxic

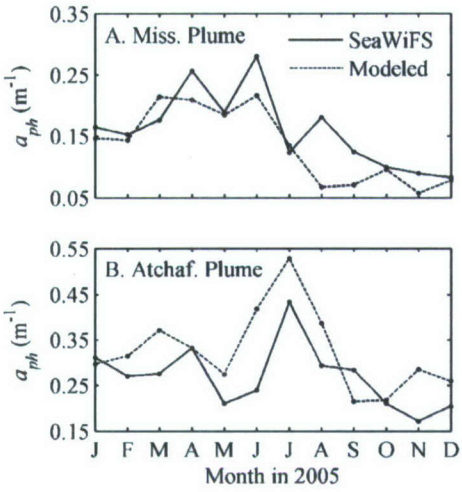

Figure 10. For 2005, time series comparisons of satellite-derived and model-predicted a_{ph} in the (a) Mississippi River plume (Box A) and (b) Atchafalaya River plume (Box B). Both satellite and modeled time series peaked in spring to early summer in the Mississippi plume and in midsummer in the Atchafalaya plume.

zone, a_{ph} often displayed wintertime peaks, and was thus negatively correlated with the two forcing variables. In deep Gulf of Mexico waters, previous studies have shown that thermally driven mixed layer depths were the main factor driving the winter maxima in phytoplankton biomass [*Walsh et al.*, 1989; *Müller-Karger et al.*, 1991]. The cooccurrence of high algal biomass, cooler SST's, and deeper mixed layers provided strong evidence that primary production in the open Gulf was controlled by the upward flux of NO_3. We hypothesize that the same thermal mechanism which controls phytoplankton growth in the open Gulf also plays a role in offshore shelf waters. Previously, studies have shown upwelling favorable currents to induce bottom Ekman upwelling that injects nutrient-rich deep water onto the shelf, causing localized high surface values of nutrients and phytoplankton biomass [*Fox et al.*, 1987; *López-Veneroni and Cifuentes*, 1994; *Sahl et al.*, 1993; *Chen et al.*, 2000]. Similarly, for our study years (2002–2004), we observed wintertime winds and currents that caused circulation to flow off-shelf, providing upwelling favorable conditions. On the basis of our study, both deeper mixed layers and favorable circulation patterns in winter appear to promote the vertical entrainment of nutrients from either benthic or upwelled sources and to increase phytoplankton biomass over the hypoxic zone. Thus, we identify two different mixing regimes on the shelf: (1) in nearer shore waters, mixing negatively affected phytoplankton biomass due to increased light limitation (Figure 6, discharge- and wind-dominated regions), and (2) farther offshore, mixing positively affected biomass due to vertical entrainment of nutrients (Figure 6, radiation- and SST-dominated regions). Similarly, multiple sources of nutrients to phytoplankton (i.e., riverine and upwelled) have been documented in other river-dominated margins, such as the Amazon River plume [e.g., *DeMaster and Pope*, 1996].

4.2. Chemical Factors Controlling Phytoplankton

[31] Over the hypoxic zone, Mississippi River nitrate concentration was one of the most important predictors of phytoplankton absorption. Riverine [NO_3] was most important in nearer shore waters (Figures 5c and 6). As in our above analysis of discharge, only two analyses of long-term in situ data sets have studied correlations between Mississippi River NO_3 and phytoplankton growth in Louisiana coastal waters. For an eight year period (1985–1992), measurements at Station C6 on the Louisiana shelf (station location shown on Figure 6) showed that primary productivity in the summertime was significantly correlated with riverine NO_3 flux lagged by one month (r = 0.73 [*Justić et al.*, 1997]). However, the authors' previous research for approximately the same years (1985–1991) and same location resulted in a higher correlation between primary productivity and discharge lagged by one month (r = 0.84

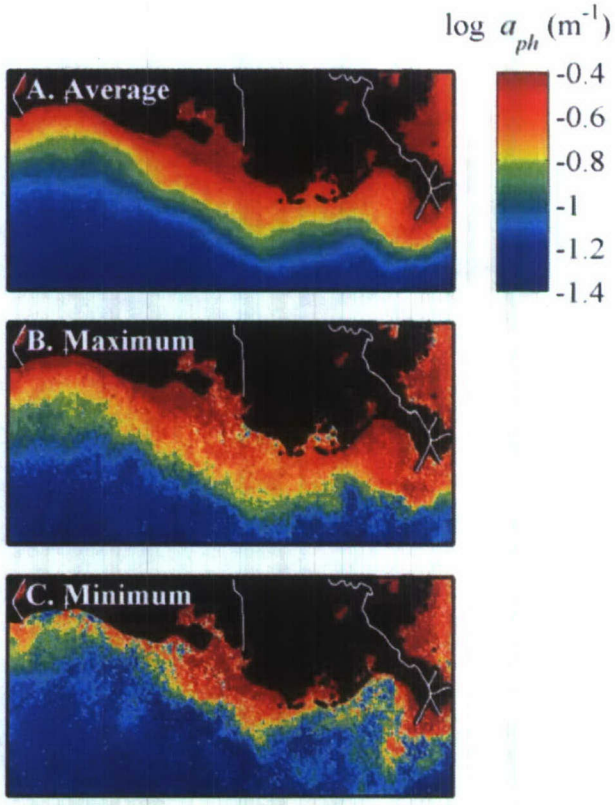

Figure 11. Spring model experiment showing variability in a_{ph} caused by changing all environmental variables, except NO_3 flux, with comparison of springtime (a) average a_{ph}, (b) maximum a_{ph}, and (c) minimum a_{ph}. Average a_{ph} was determined by inputting average springtime (April–June, 2002–2004) environmental variables into the model. Maximum and minimum a_{ph} were modeled by using the limits of all environmental variables, except NO_3 flux, during this time period. The maximum and minimum scenarios were determined on the basis of an average a_{ph} calculated over the entire region. Thus, a_{ph} may not be higher in the maximum scenario at specific locations, such as between Atchafalaya and Terrebonne Bays.

[*Justić et al.*, 1993]). Hence, we conclude that river discharge was more important than NO_3 concentration in driving productivity at station C6, in concurrence with our findings, as presented above. In contrast, *Lohrenz et al.*'s [1997] study around the delta showed that both riverine NO_3 flux and NO_3 concentration were important predictors of primary productivity during a 7-year period (1988–1994). Many of their measurements were in a region just southwest of the delta where [NO_3] was often also an important predictor of a_{ph} in our study (Figure 6). The generally good agreement between the results of our study and the limited correlations presented in previous field work is somewhat surprising. It can be difficult to directly compare results derived from point measurements to those derived from more synoptic satellite imagery, especially given differences in time period between our study and these previous measurements. As well, we are examining variability in a_{ph}, which is more an indicator of phytoplankton biomass than a rate process, such as primary production. Though, phytoplankton biomass and primary production tend to be strongly correlated in this region [*Lohrenz et al.*, 1999; *Chen et al.*, 2000].

[32] One of our main findings was that riverine nitrate concentration and river discharge were equally important determinants of a_{ph} on the shelf (Figure 6). Previous observations have demonstrated that riverine effects on salinity (and thus buoyancy and stratification) are widespread along the shelf [*Dinnel and Wiseman*, 1986], whereas riverine effects on nutrient distributions are confined closer to the river mouths [e.g., *Sahl et al.*, 1993]. In fact, we showed here that both of these chemical and physical processes are very important in determining surface phytoplankton distributions, and that their effects are observed in unique regions of the shelf – generally in nearer shore waters for [NO_3], compared to river discharge. Possible relationships with the in situ production of ammonium may help explain the importance of riverine [NO_3] away from river mouths, such as in the Atchafalaya River plume (Figures 5c and 6). On the basis of the correlation and regression analyses presented here, we also suggest that the vertical entrainment of nutrients from benthic regeneration and/or upwelled sources into surface shelf waters is regionally important to phytoplankton growth (e.g., in the more offshore region of the hypoxic zone). In the case of benthic inputs, the Mississippi and Atchafalaya Rivers may have been the initial source of these nutrients.

[33] We observed limited spatial influence of silicate and phosphate concentrations on phytoplankton absorption on the Louisiana shelf. The role of [PO_4] is somewhat less clear than that of [SiO_3], because [PO_4] was highly correlated with SST, whereas [SiO_3] generally had low correlations with other environmental forcing variables (Table 2). Our final multivariate model did not include [PO_4], but did include [SiO_3] for its role in forcing a_{ph} west of Atchafalaya Bay. Although nitrogen often controls primary production in shelf waters near the Mississippi River delta, phosphorus and silicate limitation have also been observed [e.g., *Dortch and Whitledge*, 1992; *Lohrenz et al.*, 1999]. In this study, we have only considered nutrient inputs from the Mississippi River, whereas nutrient contributions from other sources may lead to a somewhat different understanding of nutrient effects on phytoplankton. For example, processes of biological uptake, remineralization of organic matter, and/or upwelling may all affect in situ nutrient concentrations and which nutrients are limiting to growth [e.g., *Lohrenz et al.*, 1999]. However, our results should be fairly robust in nearshore waters that are directly impacted by riverine outflow. In these waters, phytoplankton biomass was the highest on the shelf and was clearly correlated with riverine [NO_3] (Figure 5c), but to only a much lesser extent with either riverine [PO_4] or [SiO_3]. Thus, we interpret our results to indicate that riverine [NO_3] is the primary nutrient controlling phytoplankton variability on the Louisiana shelf, in concurrence with previous findings [*Turner et al.*, 2006].

4.3. Implications for Management of Hypoxia

[34] Stratification and water column mixing play an important role in determining phytoplankton biomass and the areal extent of hypoxia on the Louisiana shelf. Seasonal hypoxia is the combined result of vertical stratification of the water column and respiration of surface organic carbon in bottom waters. Much attention has focused on eutrophication by increased NO_3 loading over the last 50 years as the main cause of hypoxia in Louisiana-Texas shelf bottom waters [e.g., *Turner et al.*, 2006, and references therein]. However, it is clear that physical mechanisms also strongly control the extent of hypoxia and that [NO_3] is not the sole cause. Previous work described a large region of the shelf which is affected by freshwater flow, where the euphotic zone is nitrogen limited and stratification plays the most important role in determining hypoxia [*Rowe and Chapman*, 2002]. The authors emphasized that stratification-induced hypoxia has been observed in other coastal areas (e.g., the Pamlico River Estuary [*Stanley and Nixon*, 1992]) and that Louisiana shelf hypoxia correlates just as well with the strength of the density gradient as it does with [NO_3]. Recent results from the combined use of a hydrodynamic and oxygen respiration model concluded that hypoxia formation is primarily dependent on vertical mixing processes, as determined by freshwater input, bottom topography, and winds [*Hetland and DiMarco*, 2008].

[35] Our findings further support the importance of mixing on the shelf. Although we observed spatial heterogeneity in the physical variables driving phytoplankton biomass on the shelf (Figure 6), a common factor among all of these physical variables was that their impact on phytoplankton is likely a result of changes in stratification. For example, correlation analyses showed that in nearshore and midshelf waters, lower wind speeds and increased freshwater discharge both increased phytoplankton biomass (e.g., Table 1). In offshore shelf waters, a thermally driven mixing regime was observed where we hypothesize that increased mixing in winter positively affected phytoplankton biomass due to the vertical entrainment of nutrients (Figure 6). As well, the obvious impact of mixing is observed in the passage of storms over the shelf. For example, in the years of our study, the areal extent of hypoxia was significantly reduced in years when tropical storms and hurricanes had a stronger impact on our study area (2003 and 2005, <12,000 km^2) compared to years with lower storm activity (2002 and 2004, >15,000 km^2). We also observed lower a_{ph} in July of 2003 and 2005, the years with higher wind speeds (Figures 3a and 3c).

[36] A significant degree of variability in phytoplankton biomass on the Louisiana shelf can be expected even for constant riverine NO_3 flux. A springtime experiment with our model suggested that average a_{ph} over the hypoxic zone could vary by an average 37% owing to changes in environmental variables other than NO_3 flux, and by more in some regions of the shelf (e.g., LA Bight; Figure 11). Understanding the various factors which influence hypoxia is especially important given similarity in the natural variability we observed in a_{ph} (37%) and the proposed 30% reduction in annual nitrogen flux into the Gulf of Mexico, as recommended by the Federal-State-Tribal Action Plan for reducing, mitigating, and controlling hypoxia [*Mississippi River/Gulf of Mexico Watershed Nutrient Task Force*, 2001]. The management and economic implications for reaching this nitrogen reduction goal are far-reaching, involving potential large-scale changes in agricultural fertilization practices in Midwestern states [*Mitsch et al.*, 2001]. Hence, it is important that scientists and environmental managers can explain the resulting changes in hypoxia size as nutrient flux is decreased. To the extent that there is a linkage between surface production and hypoxia, our spring model experiment suggests that changes in hypoxia size can be expected from variability in certain physical factors. For example, physical factors likely contributed to the 2002 hypoxic zone being the largest in history. In spring 2002, a year with only moderate spring-summer NO_3 concentrations (Figure 3d), we observed stronger winds and currents directed to the west, compared to either 2003 or 2004, which caused retention of freshwater and phytoplankton biomass on the shelf (Figure 8). In predictive models of hypoxia size, there is currently little consensus as to which physical processes are most important [e.g., *Scavia et al.*, 2004]. We suggest that the predictive capability of these models would be improved by incorporating some of the physical factors that we have identified as important on the shelf, especially that of water column mixing.

5. Conclusions

[37] Variability in phytoplankton biomass in Louisiana shelf surface waters is driven by a host of chemical and physical forcing variables. Of these factors, we conclude that recent variability in satellite-derived a_{ph} (2002–2004) is most strongly driven by Mississippi River discharge and riverine [NO_3], followed by SST, solar radiation, and wind speed. On the basis of these findings, two different mixing regimes were identified on the shelf, one in nearer shore waters where mixing negatively affected phytoplankton biomass due to light limitation and a second region farther offshore where mixing positively affected biomass due to upwelled nutrients. This offshore region indicates vertical entrainment as a source of nutrients to shelf phytoplankton, though likely of secondary importance to riverine nutrient inputs [e.g., *Biggs and Sanchez*, 1997]. A multiple regression model was developed from 13 of the environmental variables initially included in our analysis, and performed well in modeling spatial and temporal a_{ph} distributions in 2002–2004, as well as in predicting a_{ph} in 2005. We propose that further insights into controls on shelf phytoplankton biomass could be gained from development of seasonal models, as have been used in predicting suspended sediment distributions on the shelf [e.g., *Walker*, 1996]. As well, given inherent difficulties with satellite algorithms in coastal regions, satellite retrievals of phytoplankton biomass in this region may be further improved through the use of semianalytical algorithms [e.g., *Lee et al.*, 2002; *Maritorena et al.*, 2002], and continued validation with in situ observations. Finally, we found that the inclusion of currents from a Gulf of Mexico circulation model improved our final model for a_{ph}. We suggest that future research will benefit from improved circulation models for river-dominated shelf regions, including higher spatial resolution, incorporation of actual (rather than climatological) river inputs, and better parameterization of surface salinity flux. In summary, our findings show that time series analyses of ocean color imagery can provide valuable insights into phytoplankton dynamics in shallow shelf waters of the Gulf of Mexico. As well, we have demonstrated that remote sensing in combination with environmental forcing mechanisms may provide scientists and environmental managers with powerful tools for understanding future changes in hypoxia on the Louisiana shelf.

[38] **Acknowledgments.** This work was supported by an NRC Research Associateship award to R. Green, and NRL Program PE0601153N and NASA grant NNH04AB02I to R. Gould. We thank S. Lohrenz and R. Greene for the opportunity to participate on recent cruises and W. Goode for assistance in cruise preparation. We are also grateful to D. Ko for providing IASNFS circulation results, D. Demcheck for recent values of USGS data, and G. Stone for access to LSU WAVCIS data. Four anonymous reviewers provided insightful comments that helped to improve this manuscript.

References

Arnone, R. A., P. Martinolich, R. W. Gould Jr., M. Sydor, R. Stumpf, and S. Ladner (1998), Coastal optical properties using SeaWiFS, Meeting proceedings, Ocean Optics XIV, SPIE-The Int. Soc. for Opt. Eng., Kona, Hawaii, November.

Biggs, D. C., and L. L. Sanchez (1997), Nutrient enhanced primary productivity of the Texas-Louisiana continental shelf, *J. Mar. Syst.*, *11*, 237–247, doi:10.1016/S0924-7963(97)00019-5.

Carnes, M. R., D. N. Fox, R. C. Rhodes, and O. M. Smedstad (1996), Data assimilation in a North Pacific Ocean monitoring and prediction system, in *Modern Approaches to Data Assimilation in Ocean Modeling*, edited by P. Malanotte-Rizzoli, pp. 319–345, Elsevier, Amsterdam.

Chang, G. C., and R. W. Gould Jr. (2006), Comparisons of optical properties of the coastal ocean derived from satellite ocean color and in situ measurements, *Opt. Express*, *14*, 10,149–10,163, doi:10.1364/OE.14.010149.

Chen, X., S. E. Lohrenz, and D. A. Wiesenburg (2000), Distribution and controlling mechanisms of primary production on the Louisiana-Texas continental shelf, *J. Mar. Syst.*, *25*, 179–207, doi:10.1016/S0924-7963(00)00014-2.

Cochrane, J. D., and F. J. Kelly (1986), Low frequency circulation on the Texas-Louisiana continental shelf, *J. Geophys. Res.*, *91*, 10,645–10,659, doi:10.1029/JC091iC09p10645.

Corbett, D. R., B. McKee, and D. Duncan (2004), An evaluation of mobile mud dynamics in the Mississippi River deltaic region, *Mar. Geol.*, *209*, 91–112, doi:10.1016/j.margeo.2004.05.028.

Dagg, M. J., and T. E. Whitledge (1991), Concentrations of copepod nauplii associated with the nutrient-rich plume of the Mississippi River, *Cont. Shelf Res.*, *17*, 845–857.

Darecki, M., and D. Stramski (2004), An evaluation of MODIS and SeaWiFS bio-optical algorithms in the Baltic Sea, *Remote Sens. Environ.*, *89*, 326–350, doi:10.1016/j.rse.2003.10.012.

DeMaster, D. J., and R. Pope (1996), Nutrient dynamics in Amazon shelf waters: Results from AMASSEDS, *Cont. Shelf Res.*, *16*, 263–289, doi:10.1016/0278-4343(95)00008-O.

Dinnel, S. P., and W. J. Wiseman (1986), Freshwater on the Louisiana and Texas Shelf, *Cont. Shelf Res.*, *6*, 765–784, doi:10.1016/0278-4343(86)90036-1.

Dortch, Q., and T. E. Whitledge (1992), Does nitrogen or silicon limit phytoplankton production in the Mississippi River plume and nearby regions?, *Cont. Shelf Res.*, *12*, 1293–1309, doi:10.1016/0278-4343(92)90065-R.

D'Sa, E. J., R. L. Miller, and C. Del Castillo (2006), Bio-optical and ocean color algorithms for coastal waters influenced by the Mississippi River during a cold front, *Appl. Opt.*, *45*, 7410–7428, doi:10.1364/AO.45.007410.

Fahnenstiel, G. L., M. J. McCormick, G. A. Lang, D. G. Redalje, S. E. Lohrenz, M. Markowitz, B. Wagoner, and H. J. Carrick (1995), Taxon-specific growth and loss rates for dominant phytoplankton populations from the northern Gulf of Mexico, *Mar. Ecol. Prog. Ser.*, *117*, 229–239, doi:10.3354/meps117229.

Fox, L.-E., F. Lipschultz, L. Kerkof, and S. C. Wofsy (1987), A chemical survey of the Mississippi estuary, *Estuaries*, *10*, 1–12, doi:10.2307/1352019.

Green, R. E., G. A. Breed, M. J. Dagg, and S. E. Lohrenz (2008), Modeling the response of primary production and sedimentation to variable nitrate loading in the Mississippi River plume, *Cont. Shelf Res.*, doi:10.1016/j.csr.2007.02.008, in press.

Harding, L. W., Jr., A. Magnuson, and M. E. Mallonee (2005), SeaWiFS retrievals of chlorophyll in Chesapeake Bay and the mid-Atlantic bight, *Estuarine Coastal Shelf Sci.*, *62*, 75–94, doi:10.1016/j.ecss.2004.08.011.

Heath, M. R., K. Richardson, and T. Kiorboe (1990), Optical assessment of phytoplankton nutrient depletion, *J. Plankton Res.*, *12*, 381–396, doi:10.1093/plankt/12.2.381.

Hetland, R. D., and S. F. DiMarco (2008), How does the character of oxygen demand control the structure of hypoxia on the Texas-Louisiana continental shelf?, *J. Mar. Syst.*, *70*, 49–62, doi:10.1016/j.jmarsys.2007.03.002.

Hyde, K. J. W., J. E. O'Reilly, and C. A. Oviatt (2007), Validation of SeaWiFS chlorophyll a in Massachusetts Bay, *Cont. Shelf Res.*, *27*, 1677–1691.

Jolliff, J. K., J. C. Kindle, B. Penta, R. Helber, Z. Lee, I. Shulman, R. Arnone, and C. D. Rowley (2008), On the relationship between satellite-estimated bio-optical and thermal properties in the Gulf of Mexico, *J. Geophys. Res.*, *113*, G01024, doi:10.1029/2006JG000373.

Justić, D., N. N. Rabalais, R. E. Turner, and W. J. Wiseman Jr. (1993), Seasonal coupling between riverborne nutrients, net productivity, and hypoxia, *Mar. Pollut. Bull.*, *26*, 184–189, doi:10.1016/0025-326X(93)90620-Y.

Justić, D., N. N. Rabalais, and R. E. Turner (1997), Impacts of climate change on net productivity of coastal waters: Implication for carbon budgets and hypoxia, *Clim. Res.*, *8*, 225–237, doi:10.3354/cr008225.

Kishino, M., N. Takahashi, N. Okami, and S. Ichimura (1985), Estimation of the spectral absorption coefficients of phytoplankton in the sea, *Bull. Mar. Sci.*, *37*, 634–642.

Ko, D. S., R. H. Preller, and P. J. Martin (2003), An experimental real-time Intra Americas Sea Ocean Nowcast/Forecast System for coastal prediction, paper presented at 5th Conference on Coastal Atmospheric & Oceanic Prediction & Processes, Am. Meteorol. Soc., Boston, Mass.

Ko, D. S., P. J. Martin, C. D. Rowley, and R. H. Preller (2007), A real-time coastal ocean prediction experiment for MREA04, *J. Mar. Syst.*, *69*, 17–28, doi:10.1016/j.jmarsys.2007.02.022.

Lee, Z. P., K. L. Carder, and R. A. Arnone (2002), Deriving inherent optical properties from water color: A multiband quasi-analytical algorithm for optically deep waters, *Appl. Opt.*, *41*, 5755–5772, doi:10.1364/AO.41.005755.

Leming, T. D., and W. E. Stuntz (1984), Zones of coastal hypoxia revealed by satellite scanning have implications for strategic fishing, *Nature*, *310*, 136–138, doi:10.1038/310136a0.

Lohrenz, S. E., M. J. Dagg, and T. E. Whitledge (1990), Enhanced primary production at the plume/oceanic interface of the Mississippi River, *Cont. Shelf Res.*, *10*, 639–664, doi:10.1016/0278-4343(90)90043-L.

Lohrenz, S. E., G. L. Fahnenstiel, D. G. Redalje, G. A. Lang, X. Chen, and M. J. Dagg (1997), Variations in primary production of northern Gulf of Mexico continental shelf waters linked to nutrient inputs from the Mississippi River, *Mar. Ecol. Prog. Ser.*, *155*, 45–54, doi:10.3354/meps155045.

Lohrenz, S. E., G. L. Fahnenstiel, D. G. Redalje, G. A. Lang, M. J. Dagg, T. E. Whitledge, and Q. Dortch (1999), Nutrients, irradiance, and mixing as factors regulating primary production in coastal waters impacted by the Mississippi River plume, *Cont. Shelf Res.*, *19*, 1113–1141, doi:10.1016/S0278-4343(99)00012-6.

López-Veneroni, D., and L. A. Cifuentes (1994), Transport of dissolved organic nitrogen in Mississippi River plume and Texas-Louisiana continental shelf near-surface waters, *Estuaries*, *17*, 796–808, doi:10.2307/1352748.

Maritorena, S. and J. O'Reilly (2000), Update on the initial operational SeaWiFS chlorophyll *a* algorithm, in *SeaWiFS Postlaunch Technical Report Series*, vol. 11, edited by S. B. Hooker and E. R. Firestone, *NASA Tech. Memo.*, *1999-206892*, 3–9.

Maritorena, S., D. A. Siegel, and A. R. Peterson (2002), Optimization of a semianalytical ocean color model for global-scale applications, *Appl. Opt.*, *41*, 2705–2714, doi:10.1364/AO.41.002705.

Martin, P. J. (2000), Description of the Navy Coastal Ocean Model Version 1.0, Tech. Rep. NRL/FR/7322-00-9962, 42 pp., Naval Res. Lab., Washington, D. C.

Martinolich, P. M. (2005), *Automated Processing System User's Guide Version 3.4*, Naval Res. Lab., Washington, D. C. (Available at http://www7333.nrlssc.navy.mil/docs/aps_v3.4/user/aps/)

Mississippi River/Gulf of Mexico Watershed Nutrient Task Force (2001), *Action plan for reducing, mitigating, and controlling hypoxia in the northern Gulf of Mexico, report, Off. of Wetlands, Oceans, and Watersheds*, U.S. Environ. Prot. Agency, Washington, D. C.

Mitchell, G., et al. (2000), Determination of spectral absorption coefficients of particles, dissolved material and phytoplankton for discrete water samples, Ocean Optics Protocols for Satellite Ocean Color Sensor Validation Revision 2, edited by G. S. Fargion and J. L. Mueller, *NASA Tech. Memo.*, *NASA/TM-2000-209966*, 125–153.

Mitsch, W. J., J. W. Day Jr., J. W. Gilliam, P. M. Groffman, D. L. Hey, G. W. Randall, and N. Wang (2001), Reducing nitrogen loading to the Gulf of Mexico from the Mississippi River basin: Strategies to counter a persistent ecological problem, *Bioscience*, *51*, 373–388, doi:10.1641/0006-3568(2001)051[0373:RNLTTG]2.0.CO;2.

Müller-Karger, F. E., J. J. Walsh, R. H. Evans, and M. B. Meyers (1991), On the seasonal phytoplankton concentration and sea surface temperature cycles of the Gulf of Mexico as determined by satellites, *J. Geophys. Res.*, *96*, 12,645–12,665, doi:10.1029/91JC00787.

Neori, A., O. Holm-Hansen, B. G. Mitchell, and D. A. Kiefer (1984), Photoadaptation in marine phytoplankton-Changes in spectral absorption and excitation of chlorophyll-a fluorescence, *Plant Physiol.*, *76*, 518–524.

Rabalais, N. N. and R. E. Turner (2006), Oxygen depletion in the Gulf of Mexico adjacent to the Mississippi River, in *Past and Present Marine Water Column Anoxia*, *NATO Sci. Ser.*, vol. 4, edited by L. N. Neretin, pp. 225–245, Springer, New York.

Rabalais, N. N., R. E. Turner, and W. J. Wiseman Jr. (2002), Gulf of Mexico hypoxia, a.k.a. "The Dead Zone", *Annu. Rev. Ecol. Syst.*, *33*, 235–263, doi:10.1146/annurev.ecolsys.33.010802.150513.

Ransibrahmanakul, V., and R. P. Stumpf (2006), Correcting ocean colour reflectance for absorbing aerosols, *Int. J. Remote Sens.*, *27*, 1759–1774, doi:10.1080/01431160500380604.

Redalje, D. G., S. E. Lohrenz, and G. L. Fahnenstiel (1994), The relationship between primary production and the vertical export of particulate organic matter in a river-impacted coastal ecosystem, *Estuaries*, *17*, 829–836, doi:10.2307/1352751.

Rowe, G. T., and P. Chapman (2002), Continental shelf hypoxia: Some nagging questions, *Gulf Mex. Sci.*, *20*, 153–160.

Sahl, L. E., W. J. Merrell, and D. C. Biggs (1993), The influence of advection on the spatial variability of nutrient concentrations on the Texas-Louisiana continental shelf, *Cont. Shelf Res.*, *13*, 233–251, doi:10.1016/0278-4343(93)90108-A.

Salisbury, J. E., J. W. Campbell, E. Lindner, L. D. Meeker, F. E. Muller-Karger, and C. J. Vorosmarty (2004), On the seasonal correlation of surface particle fields with wind stress and Mississippi discharge in the northern Gulf of Mexico, *Deep Sea Res., Part II*, *51*, 1187–1203.

Scavia, D., D. Justić, and V. J. Bierman Jr. (2004), Reducing hypoxia in the Gulf of Mexico: Advice from three models, *Estuaries*, *27*, 419–425.

Siegel, D. A., M. H. Wang, S. Maritorena, and W. Robinson (2000), Atmospheric correction of satellite ocean color imagery: The black pixel assumption, *Appl. Opt.*, *39*, 3582–3591.

Stanley, D. W., and S. W. Nixon (1992), Stratification and bottom-water hypoxia in the Pamlico River estuary, *Estuaries*, *15*, 270–281, doi:10.2307/1352775.

Stumpf, R. P., R. A. Arnone, R. W. Gould, P. Martinolich, V. Ransibrahmanakul, P. A. Tester, R. G. Steward, A. Subramaniam, M. Culver, and J. R. Pennock (2000), SeaWiFS ocean color data for US Southeast coastal waters, paper presented at Sixth International Conference on Remote Sensing for Marine and Coastal Environments, ERIM Intl., Charleston, S. C.

Stumpf, R. P., R. A. Arnone, R. W. Gould Jr., P. M. Martinolich, and V. Ransibrahmanakul (2003), A partially-coupled ocean-atmosphere model for retrieval of water-leaving radiance from SeaWiFS in coastal waters, in *Algorithm Updates for the Fourth SeaWiFS Data Reprocessing*, vol. 22, edited by S. B. Hooker et al., *NASA Tech. Memo.*, *2002-206892*, 51–59.

Turner, R. E., N. N. Rabalais, and D. Justić (2006), Predicting summer hypoxia in the northern Gulf of Mexico: Riverine N, P, and Si loading, *Mar. Pollut. Bull.*, *52*, 139–148, doi:10.1016/j.marpolbul.2005.08.012.

Walker, N. D. (1996), Satellite assessment of Mississippi River plume variability: Causes and predictability, *Remote Sens. Environ.*, *58*, 21–35, doi:10.1016/0034-4257(95)00259-6.

Walsh, J. J., D. A. Dieterle, M. B. Meyers, and F. E. Müller-Karger (1989), Nitrogen exchange at the continental margin: A numerical study of the Gulf of Mexico, *Prog. Oceanogr.*, *23*, 245–301, doi:10.1016/0079-6611(89)90002-5.

Yuan, J. C., M. J. Dagg, and C. E. Del Castillo (2005), In-pixel variations of chl a fluorescence in the Northern Gulf of Mexico and their implications for calibrating remotely sensed chl a and other products, *Cont. Shelf Res.*, *25*, 1894–1904, doi:10.1016/j.csr.2005.06.003.

R. W. Gould Jr. and R. E. Green, Ocean Optics Section, Code 7333, Naval Research Laboratory, Stennis Space Center, Mississippi 39529, USA. (gould@nrlssc.navy.mil; rgreen@nrlssc.navy.mil)